Nucleation Initiated Spinodal Decomposition in a Polymerizing System

Thein Kyu and Jae-Hyung Lee
Institute of Polymer Engineering, The University of Akron, Akron, Ohio 44325
(Received 29 September 1995)

Dynamics of phase separation in a polymerizing system, consisting of carboxyl terminated polybutadiene acrylonitrile/epoxy/methylene dianiline, was investigated by means of time-resolved light scattering. The initial length scale was found to decrease for some early periods of the reaction which has been explained in the context of nucleation initiated spinodal decomposition. We have combined the Cahn-Hilliard kinetic equation and polymerization kinetics, and predicted the initial reduction of the length scale triggered by nucleation. [S0031-9007(96)00155-X]

PACS numbers: 61.41.+e, 64.60.Cn, 64.75.+g

In recent years, polymerization-induced phase separation in thermoset-thermoplastic blends have gained renewed interest because of unusual equilibrium and nonequilibrium pattern formations [1–6]. Liquid-liquid phase separation generally occurs in those polymer blends due to polymerization [1–6] or thermal quenching into an unstable region from an initially homogeneous state [7–13]. While thermally induced phase separation has been well investigated for quenched binary systems, there are limited studies on the problem of phase separation driven by polymerization, although it may be equally, if not more, important [1–6].

When a polymer blend is brought from an initially homogeneous state into an unstable spinodal region, various modes of concentration fluctuations develop and are amplified simultaneously by virtue of thermal fluctuations [7,8], causing the two-phase structure to be irregular. However, if thermal fluctuation is suppressed fully, a single selective mode grows predominantly such that the structure becomes more regular. In the latter case of reaction-induced phase separation, instability of the system is driven by the progressive increase of molecular weight of the polymerizing species. Once the condensation reaction has been initiated, the nonequilibrium structure will emerge in a manner dependent on competition between reaction kinetics and phase separation dynamics. The understanding of the governing mechanisms of polymerization-induced phase separation is of paramount importance in elucidating development of final morphology.

In the present paper, polymerization-induced phase separation has been investigated for a mixture of bisphenol-A diglycidyl ether (BADGE) epoxy, commercially known as EPON 828, and carboxyl terminated butadiene acrylonitrile (CTBN) by using methylene dianiline (MDA) as a curing agent. Here, "polymerization" refers to a condensation reaction which gives rise to linear chains, whereas "curing" (or cross-linking) implies a chain branching reaction leading to a three dimensional network. BADGE and CTBN were codissolved in tetrahydrofuran (THF) at a polymer concentration of 10 wt/vol%. An equivalent amount of MDA was subsequently added to the solution mixtures. Thin films ($\sim 10\ \mu$m thick) were solvent cast and then dried in a vacuum oven at ambient temperature for 1–4 h to remove residual solvent. These films were completely transparent, suggestive of miscibility at least at the length scale of the wavelength of light. The blend films were polymerized in a time-resolved light scattering apparatus [10] by subjecting the films to various reaction temperatures in order to vary the relative rates of phase separation and polymerization. Temporal evolution of scattering profiles were monitored to probe dynamics of phase separation in both 10/90/23.5 and 20/80/21 CTBN/BADGE/MDA compositions.

Figures 1(a) and 1(b) show a typical time evolution of scattered intensity versus scattering wave number (q) at the 10/90/23.5 and 20/80/21 CTBN/BADGE/MDA compositions during polymerization, where q is defined as $q = (4\pi/\lambda)\sin\theta/2$; θ and λ are the scattering angle and the wavelength of light measured in the medium. The scattering maximum (q_m) develops first around 3 μm^{-1}, then moves to a larger scattering angle which is contrary to our intuition or general perception. Figure 2(a) shows the plot of q_m versus time for the 10/90/23.5 composition at various temperatures. The average length scale initially decreases, then levels off at all temperatures investigated. Multiple tiny droplets can be seen in the entire microscopic view, but it is difficult to differentiate

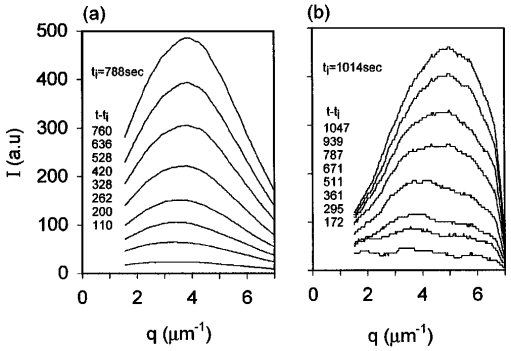

FIG. 1. Time evolution of scattering profiles phase separation driven by polymerization of (a) 10/90/23.5 at 80 °C and (b) 20/80/21 CTBN/BADGE/MDA at 50 °C.

 0031-9007/96/76(20)/3746(4)$10.00

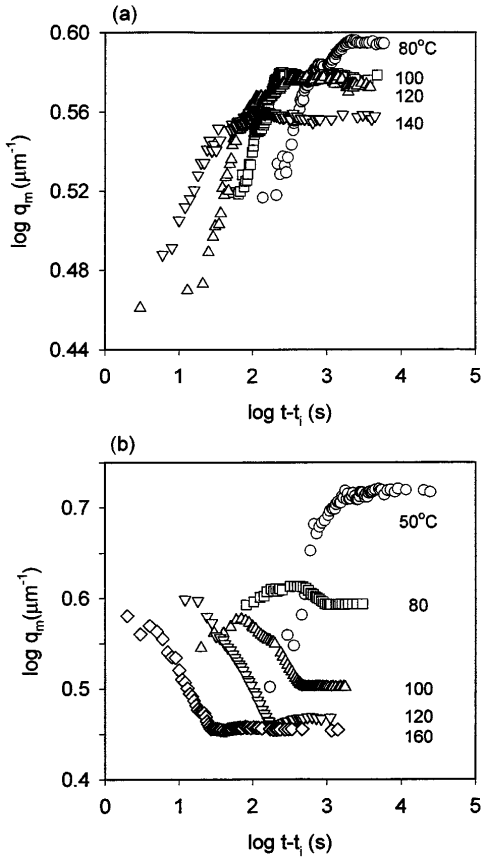

FIG. 2. q_m vs $t^{-\alpha}$ plots at various reaction temperature following phase separation driven by polymerization of (a) 10/90/23.5 and (b) 20/80/21 CTBN/BADGE/MDA.

any subtle variation of the domain size under the microscopic investigation. The initial decrease of the length scale can be confirmed in the light scattering experiments following condensation polymerization of the 20/80/21 composition at 50 °C. A similar observation was made at 80 °C, but the domains coarsen at a later stage [Fig. 2(b)]. At higher reaction temperatures of 100, 120, and 140 °C, the growth process becomes more pronounced as the mutual diffusion is expedited at elevated temperatures more rapidly than the reaction kinetics. Finally, the domains cease to grow when the cross-linking reaction takes place. The initial reduction of the length scale is not observable if phase separation is faster than the reaction, viz. the coarsening process is dominant. This peculiar phenomenon may be explained in terms of a "domain insertion model" which suggests that newer domains are created in the interdomain regions of the preformed domains, leading to the smaller interdomain distances. It should be pointed out that the observed interference scattering peak cannot be expected for a conventional heterogeneous nucleation unless the nucleation is coupled with spinodal decomposition during progressive polymerization.

Figure 3 depicts the calculated temporal change of an upper critical solution temperature (UCST) curve with increasing molecular weight of the epoxy due to condensation polymerization. The UCST curve at $t = t_1$ was obtained from the cloud point phase diagram of the CTBN/BADGE blends without utilizing a curing agent [10]. When MDA was added to the CTBN/BADGE mixtures, all samples revealed optical clarity to the naked eye, suggesting that the UCST has been suppressed below room temperature. As polymerization proceeds, the molecular weight increases progressively, resulting in the shift of the UCST peak to a higher temperature as well as to a higher CTBN composition. When the coexistence curve surpasses the reaction temperature, nucleation occurs in the metastable region bound by the coexistence curve and the spinodal line. Subsequently, newer domains are formed in the interdomain region, resulting in the decrease of the average interdomain distances. This trend is observed at the 10/90/23.5 composition in all isothermal reaction temperatures. Since the UCST maximum shifts progressively to higher CTBN compositions, the reaction temperatures seemingly remain in the metastable region. In the case of the 20/80/21 composition, the polymerization temperatures are located on the other side of the UCST peak. When the reaction temperature of 80 °C moves gradually from the metastable to the unstable region, the nucleation takes place initially in the metastable region and then crosses over to the spinodal region. However, the reactions at the higher temperatures fall quickly into an unstable spinodal region due to the fast polymerization, and, eventually, the domains cease to grow as curing begins. This crossover behavior of phase separation from the metastable to the unstable region driven by polymerization may be called "nucleation initiated spinodal decomposition (NISD)."

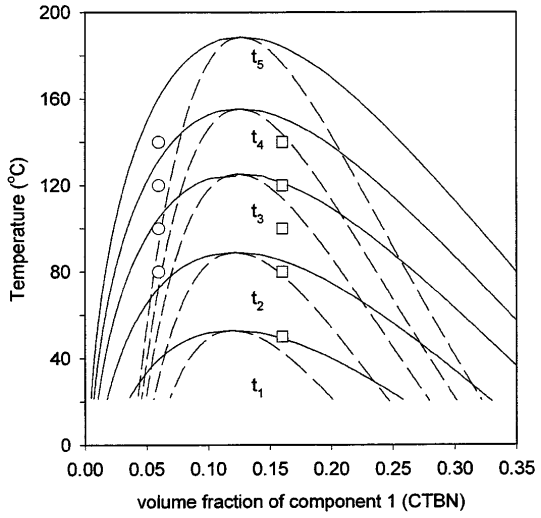

FIG. 3. Time-dependent UCST associated with progressive polymerization of epoxy in the CTBN/BADGE/MDA mixture. The UCST at $t = t_1$ was estimated from the cloud point phase diagram of CTBN/BADGE without using a curing agent (Ref. [10]).

To elucidate the origin of the NISD process, we have incorporated the reaction kinetics into the time-dependent Cahn-Hilliard equation for describing the dynamics of phase separation induced by polymerization. The total free energy of the system (ΔF) may be expressed in terms of a local free energy density, $f(\phi)$, and the gradient of concentration fluctuations, $\nabla\phi$ [7], i.e.,

$$\frac{\Delta F}{k_B T} = \int dr\left\{ f[\phi(r)] + \frac{a^2}{36\phi(1-\phi)}[\nabla\phi]^2\right\}, \quad (1)$$

where k_B is the Boltzmann constant, T the absolute temperature, ϕ the volume fraction of component 1 (CTBN), and a the correlation length which is equal to Kuhn's statistical segmental length of individual component (a_1 and a_1), assuming that $a_1 = a_2$ [11,12]. The local free energy density is given customarily by the Flory-Huggins equation, i.e.,

$$f(\phi) = \frac{\phi}{N_1}\ln\phi + \frac{1-\phi}{N_2}\ln(1-\phi) + \chi\phi(1-\phi), \quad (2)$$

where N_1 and N_2 are the degrees of polymerization of CTBN and epoxy, respectively. Away from equilibrium, the diffusion current is driven by the gradient of chemical potential, $\nabla\mu$ [7]. Combining with the continuity equation, one obtains

$$\frac{\partial\phi(r,t)}{\partial t} = -\nabla J(r,t) = \nabla\frac{\Lambda(\phi)}{k_B T}\nabla\mu, \quad (3)$$

where $\mu = \delta\Delta F/\delta\phi$ and Λ is the Onsager coefficient which may be expressed in the context of the Rouse model [12,13] as $\Lambda = a^2 W\phi(1-\phi)$. For slow spatial variation, the contribution from the gradient term is generally small relative to other contributions, and thus the square of the gradient term may be ignored [12]. This eventually leads to

$$\frac{\partial\phi}{\partial t} = \nabla\left(a^2 W\phi(1-\phi)\nabla\left[\frac{\ln\phi+1}{N_1} - \frac{\ln(1-\phi)+1}{N_2} + \chi(1-2\phi) - \frac{a^2}{18\phi(1-\phi)}\nabla^2\phi\right]\right), \quad (4)$$

where W is the rate of segmental motion. In the present system, the molecular weight of the polymerizing component (i.e., N_2) increases with progressive reaction.

Let us first consider an idealized condensation polymerization in mixtures of CTBN and BADGE with MDA. The extent of reaction (i.e., the functional sites reacted relative to the total functional groups) p for an equivalent amount of BADGE and MDA functional groups may be defined according to Carother's equation:

$$P = \frac{2(M_0 - M)}{M_0 f_{\text{avg}}}, \quad (5)$$

where the average functional groups may be defined as $f_{\text{avg}} = \sum M_j f_j / \sum M_j$, in which M_j is the number of molecules of monomer j having functionality f_j, M_0 the number of monomer molecules present initially, and M the resulting number of molecules after the reaction has occurred. The degree of polymerization of epoxy can be defined as $N_2 = M_0/M$. For a BADGE/MDA system under consideration, the degree of conversion p can be related to the degree of polymerization N_2 as

$$p(t) = \frac{2}{f_{\text{avg}}}\left(1 - \frac{1}{N_2(t)}\right). \quad (6)$$

We expressed Eq. (6) in a time-dependent form because the degree of conversion increases with reaction time, so does the degree of polymerization. In principle, p is maximized at $2/f_{\text{avg}}$, although a complete conversion cannot be expected for any condensation reactions [14], particularly for the present CTBN/BADGE/MDA system. For an idealized case, the rate of condensation polymerization may be expressed as

$$\frac{dp(t)}{dt} = k\{1 - p(t)\}^n, \quad (7)$$

where k has a usual Arrhenius form, viz., $k = A\exp(-E/k_B T)$ and n is the kinetic exponent [15]. A common feature with many epoxy systems is that the curing process is an autocatalytic reaction; i.e., the hydroxyl groups formed as a result of the reaction between the primary amine and epoxide group catalyze the reaction between the secondary amine and epoxide [14]. If this secondary reaction were to involve in the CTBN/BADGE/MDA, Eq. (7) may be modified as follows [15]:

$$\frac{dp(t)}{dt} = k' p(t)^m [1 - p(t)]^n. \quad (8)$$

This kind of secondary reaction is generally extremely slow relative to the primary reaction.

If the chemical reaction is faster than the phase separation, the domains will be frozen-in at some early stages of decomposition, in which case Eq. (5) may be linearized by taking into consideration the concentration fluctuations (or order parameter), viz., $\delta\phi = \phi - \phi_0$. This eventually leads to the linearized Cahn-Hilliard equation, which has been extensively used for describing the early stage of spinodal decomposition:

$$\frac{\partial\delta\phi(t)}{\partial t} = a^2 W\phi_0(1-\phi_0)\nabla^2\left(\frac{1}{N_1\phi_0} + \frac{1}{N_2(t)(1-\phi_0)} - 2\chi - \frac{a^2\nabla^2}{18\phi_0(1-\phi_0)}\right)\delta\phi. \quad (9)$$

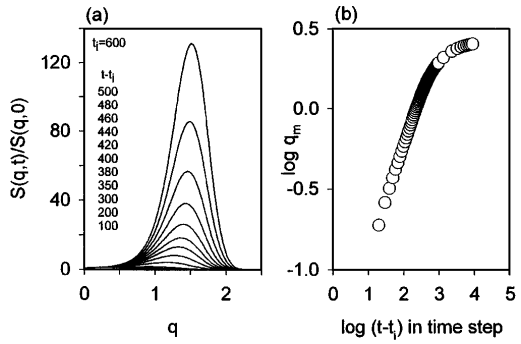

FIG. 4. (a) Temporal change of calculated structure factors for the case of $m = 1$, $n = 1$ by setting $k = 0.01$, $\phi_0 = 0.1$, $\sigma = 0.35$, $\chi = 0.615$, $T = 100\,^{\circ}\mathrm{C}$, $N_1 = 54$, and (b) the corresponding phase growth in time steps.

Rewriting Eq. (9) in Fourier space, one obtains the structure factor $S(q, t)$, i.e.,

$$\frac{S(q,t)}{S_q(0)} = \exp\left\{ -2a^2 W \phi_0 (1 - \phi_0) q^2 \times \left[\frac{t}{N_1 \phi_0} + \int \frac{dt}{N_2(t)(1 - \phi_0)} - 2\chi t + \frac{a^2 q^2 t}{18\phi_0(1 - \phi_0)} \right] \right\}, \quad (10)$$

where $S_q(0)$ is the structure factor at $t = 0$. Equation (10) may be solved analytically for a simple primary reaction ($m = 0$, $n = 1$) or that involving a secondary reaction (e.g., $m = 1$, $n = 1$), but there is no analytical solution for noninteger m and n.

Strictly speaking, a_1 may not be equal to a_2 in the real system, hence a^2 should be replaced by $a_1^2\phi + a_2^2(1 - \phi)$ in Eq. (10). However, the final outcome will not be affected because the time-dependent structure factor was calculated at a fixed composition, where a_1 and a_2 are constants. In the initial stage of reaction-driven phase separation, the condensation reaction is most likely to be linear, thus f_{avg} may be taken as 2 in the calculation. Figure 4(a) illustrates the temporal change of structure factor calculated according to Eq. (10) by setting $m = 1$, $n = 1$, and the extent of reaction at $t = 0_i$, $p_0 = 0.001$. The peak of the structure factor shifts to higher scattering angles with reaction time which may be ascribed to the decreases of average interdomain distance associated with progressive polymerization. It is apparent that the theoretical prediction [Fig. 4(b)] captures the experiment trends of all reaction temperatures in the 10/90/23.5 and of the low reaction temperatures at the 20/80/21 CTBN/BADGE/MDA composition [Figs. 2(a) and 2(b)].

In summary, we have demonstrated that the initial reduction in the length scale is triggered by nucleation during polymerization. The crossover behavior of phase separation from the metastable to the unstable states may be attributed to the nucleation initiated spinodal decomposition in the present polymerizing system. Our linear analysis on the early stage of polymerization-induced phase separation correctly predicted this NISD behavior.

Partial support of this work by the NSF, Science and Technology Center for ALCOM under Grant No. 89-20147 is gratefully acknowledged.

[1] K. Yamanaka, Y. Takagi, and T. Inoue, Polymer **60**, 1839 (1989).
[2] H. Tanaka, T. Suzuki, T. Hayashi, and T. Nishi, Macromolecules **25**, 4453 (1992).
[3] J. Y. Kim, C. H. Cho, P. Palffy-Muhoray, M. Mustafa, and T. Kyu, Phys. Rev. Lett. **71**, 2232 (1993).
[4] A. Imagawa and Q. Tran-Cong, Macromolecules **28**, 8388 (1995).
[5] H. Furukawa, J. Phys. Soc. Jpn. **63**, 3744 (1994).
[6] S. C. Glotzer and A. Coniglio, Phys. Rev. E **50**, 4241 (1994).
[7] J. D. Gunton, M. San Miguel, and P. S. Sahni, in *Phase Transitions and Critical Phenomena*, edited by C. Domb and J. L. Lebowitz (Academic Press, New York, 1983).
[8] H. E. Cook, Acta Metall. **18**, 297 (1970).
[9] J. W. Cahn and J. E. Hilliard, J. Chem. Phys. **28**, 258 (1958).
[10] H. S. Lee and T. Kyu, Macromolecules **23**, 459 (1990).
[11] P. de Gennes, J. Chem. Phys. **72**, 4756 (1980); P. Pincus, J. Chem. Phys. **75**, 1996 (1981).
[12] K. Binder, J. Chem. Phys. **79**, 6387 (1983).
[13] M. A. Kotnis and M. Muthukumar, Macromolecules **25**, 1716 (1992).
[14] G. Odian, *Principles of Polymerization* (Wiley-Intersciences, New York, 1981), 2nd ed.
[15] M. E. Ryan and A. Dutta, Polymer **20**, 203 (1979).